IEEE Access
Multidisciplinary | Rapid Review | Open Access Journal

Received 26 August 2022, accepted 8 September 2022, date of publication 12 September 2022, date of current version 10 November 2022.

Digital Object Identifier 10.1109/ACCESS.2022.3206006

RESEARCH ARTICLE

A Reliable Singular Value Decomposition and Geometric Mean Decomposition Based Precoding Scheme for MU-MIMO-VLC System

WENDUO QIU, YAN FENG, AND YOU ZHANG
School of Information Science and Technology, Tibet University, Lhasa 850000, China
Corresponding author: Yan Feng (fy4528@163.com)

This work was supported by the Project of National Natural Science Foundation of China under Grant U20A20162.

ABSTRACT In this paper, in order to improve the reliability of Multi-User Multiple-Input Multiple-Output Visible Light Communication (MU-MIMO-VLC) system, we propose a precoding scheme that based on Singular Value Decomposition (SVD) and Geometric Mean Decomposition (GMD) assisted Orthogonal Transformation (OT). In this design, we use SVD to conduct the decomposition of the user's complementary channel matrix. Then, the equivalent channel matrix is obtained by multiplying the user's channel matrix and the decomposed component. After that, the GMD is carried out to decompose the equivalent channel matrix. Finally, the precoding matrix of the proposed scheme is obtained. We then derive the theoretical Symbol Error Rate (SER) of the proposed scheme. The simulation results are provided to validate the effectiveness of the proposed scheme, and to demonstrate that the reliability of the proposed design is superior to benchmark schemes.

INDEX TERMS Multiple-input multiple-output, multi-user visible light communication, singular value decomposition, geometric mean decomposition, reliability.

DESCRIPTIONS OF SYMBOLS AND ABBREVIATIONS

$(\cdot)^*$	Conjugate transpose.
$(\cdot)!$	The factorial operation.
β_v	Atmospheric extinction coefficient.
η	SNR.
exp	Exponential operation.
$\Gamma(\cdot)$	Gamma function.
ln	Logarithmic operation.
$\overline{\mathbf{H}}_{i,GMD}$	The equivalent channel matrix of user i that is decomposed by GMD.
$\overline{\mathbf{H}}_{i,SVD}$	The equivalent channel matrix of user i that is decomposed by SVD.
$\overline{H}_i$	The equivalent channel matrix $\overline{H}_i$ of user i.
$\Phi_{1/2}$	Divergence semi-angle of transmitters.
$\Psi_{1/2}$	Field of view (FOV) semi-angle of receiver.
sec	Secant trig functions.
σ^2	Mean square slope of the sea surface.
σ_{lt}^2	Logarithmic irradiation variance.
$\sum$	Summation
tan	Tangent trig operation.
$\mathbf{F}_{i,SVD}$	Precoding matrix of user i generated by the double SVD scheme.
$\mathbf{F}_{i,SVDandGMD}$	Precoding matrix of user i generated by the SVD and GMD scheme.
Θ	Scattering angle.
θ_p	Polar angle.
$\widetilde{H}_i$	The complementary channel matrix $\widetilde{H}_i$ of user i.
ξ, γ	The parameters describing the turbulence experienced by waves.
A	LED receiving aperture area.
$B_{\xi-\gamma}(\cdot)$	$\xi - \gamma$ order second kind of modified Bessel function.

The associate editor coordinating the review of this manuscript and approving it for publication was Walid Al-Hussaibi.

c	Photoelectric conversion efficiency.
C_n^2	A parameter used to describe the turbulence intensity.
D	LED receiving aperture diameter.
E_s	Signal energy.
h	The channel coefficient.
h_p	Path fading.
$h_{t,s}$	The channel coefficient of strong turbulence.
$h_{t,w}$	The channel coefficient of weak turbulence.
h_t	Turbulent fading.
$I(\cdot,\cdot,\cdot)$	Coefficient of $B_{\xi-\gamma}(\cdot)$.
k	Phase constant.
$L_{a,u}$	Distance of the propagation link.
m	The total number of users.
N_0	Noise power.
N_r	Sum of the number of LED receiving apertures $N_{r,i}$ for each user i.
N_t	Total number of LED transmission apertures.
$Q(\cdot)$	Error complementary function.
s_r	Separation distance between receivers.
s_t	Separation distance between transmitters.
V	Wind speed.
$Z(\cdot,\cdot)$	The Lah numbers.
DC	Direct Current.
FOC	Free-space Optical Communication.
FOV	Field of view.
GMD	Geometric Mean Decomposition.
ISM	Industrial, Scientific, and Medical.
LED	Light-Emitting Diode.
MC	Monte Carlo.
MIMO	Multiple-Input Multiple-Output.
MU-MIMO-VLC	Multi-User Multiple-Input Multiple-Output Visible Light Communication.
MUIs	Multi-User Interferences.
OT	Orthogonal Transformation.
OWC	Optical Wireless Communication.
PAM	Pulse Amplitude Modulation.
PEP	Pairwise Error Probability.
RF	Radio Frequency.
SER	Symbol Error Rate.
SM	Spatial Modulation.
SMP	Spatial MultiPlexing.
SNR	Signal-to-Noise Ratio.
STBC	Space-Time Block Code.
SVD	Singular Value Decomposition.
SVD-GMD-OT	Singular Value Decomposition (SVD) and Geometric Mean Decomposition (GMD) assisted Orthogonal Transformation (OT).
SVD-OT	Double SVD assisted OT.
UCD	Unified Channel Decomposition.
VLC	Visible Light Communication.

I. INTRODUCTION

In the traditional Radio Frequency (RF) communication, spectrum resources are limited as a natural resource. Along with the increasing applications of wireless user equipments, the public Industrial, Scientific, and Medical (ISM) bands are becoming more and more crowded, resulting in insufficient available bandwidth, increasing interferences, and worse reliability [1]. Therefore, traditional RF communication cannot meet people's requirements for communication quality. Hence, in recent years, except for the efforts of exploiting the resources in the spectral domain, the resources in the space domain are also utilized to improve the transmission performance. For example, Multiple-Input Multiple-Output (MIMO) technologies have been widely applied to improve the transmission rate or the reliability by respectively utilizing the spatial multiplexing or the spatial diversity gain [2], [3], [4], [5], [6], [7].

MIMO communication utilizes space resources and changes the number of antennas at the receiving end and the transmitting end [8]. MIMO technology is not only widely used in the RF field, but also has been applied by researchers to many other scenarios [9]. And researchers also develop many technologies that can be applied on the basis of this technology, such as diversity coding, precoding [10] etc. In recent years, MIMO precoding technologies have been widely studied, such as Singular Value Decomposition (SVD), Geometric Mean Decomposition (GMD), Unified Channel Decomposition (UCD) and Space-Time Block Code (STBC) [11], [12].

To further utilize the broad bandwidth of the optical spectrum band, researchers have proposed to apply the Optical Wireless Communication (OWC) technology for information transmissions, wherein the Light-Emitting Diodes (LEDs) are used instead of antennas to transmit the user data and have been used in Free-space Optical Communication (FOC) [13], [14]. The OWC has the following merits for delivering the user data: 1) the optical bandwidth is large; 2) the electromagnetic interference is relatively low in underwater communications [15], [16]; 3) user data are transmitted by adjusting the brightness of the LEDs [17].

Nowadays, LED lighting is mostly composed of a large number of single LED lamps, which can compose massive MIMO [18] system to provide transmission services for multiple users in Visible Light Communication (VLC) system. In order to further improve the reliability of Multi-User MIMO Visible Light Communication (MU-MIMO-VLC) system, the optimal coding technologies are presented, such as Spatial Modulation (SM) [10], [12], [19] scheme, Spatial MultiPlexing (SMP) [1], [19], [20] scheme, and Orthogonal Transformation (OT) [19] scheme.

For MU-MIMO-VLC system, the precoding scheme has been proposed to provide the following advantages: the

full spatial diversity gain; the array LED gain; strong anti-interference performance; low complexity; easy hardware implementation; being compatible with current wireless communication system; easy to integrate with other technologies. For example, the precoding matrix generated by the double SVD has been used for the precoding [20]. The precoding matrix is generated by the complementary channel matrix and the equivalent channel matrix. This scheme can reduce Multi-User Interferences (MUIs). In addition, the precoding matrix generated by GMD is also proposed for the precoding [21], since each sub-channel has the same Signal-to-Noise Ratio (SNR) and the complex bit allocation procedure is removed.

In this paper, a precoding scheme based on SVD and GMD assisted OT (SVD-GMD-OT) is proposed for the MU-MIMO-VLC system to improve the reliability. In this design, the user data are first modulated and encoded by the Pulse Amplitude Modulation (PAM) and OT. Then, the SVD operation is performed on the complementary channel matrix, and GMD is used to decompose the equivalent channel matrix. Therefore, the proposed scheme not only inherits the advantages of suppressing the interference but also removes the complex bit allocation operations. Note that the OT is applied to expand the Euclidean distance between different symbols. Subsequently, we derive the theoretical Symbol Error Rate (SER) of the proposed scheme. Then the simulation results verify that the proposed scheme can effectively improve the reliability.

Briefly the major contributions include:

1) A precoding scheme based on SVD and GMD is proposed to improve the reliability for MU-MIMO-VLC system.
2) We derive the theoretical SER expression for the proposed transceiver.
3) Simulated results are provided to verify the effectiveness of the proposed scheme, and that the proposed MIMO transmission system can achieve higher reliability.

The rest of this paper is organized as follows. Section II introduces the structure of the MU-MIMO-VLC system and the precoding scheme based on SVD and GMD proposed in this paper. Section II-C briefly describes several channel environments used in this paper. Section III presents the SER analysis of the proposed scheme. The simulation results are provided in Section IV, and Section V concludes the findings.

II. MU-MIMO-VLC SYSTEM BASED ON SVD AND GMD PRECODING

In this section, we will introduce the transmitter and receiver structure of MU-MIMO-VLC system which uses the precoding scheme based on SVD-GMD proposed in this paper, and the channel models applied in this scheme.

A. TRANSMITTER

The transmitter structure of the MU-MIMO-VLC system is shown in Fig. 1. Each user data are modulated and encoded

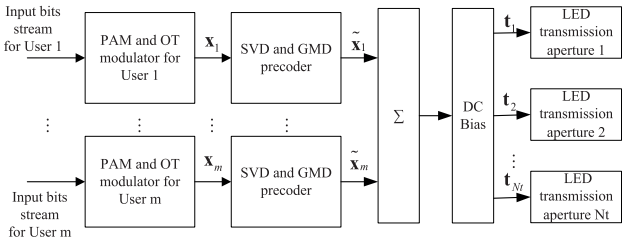

FIGURE 1. Transmitter structure.

independently in parallel. Take the user i as an example, the data will be first modulated and encoded by PAM and OT to obtain $\mathbf{x}_i$.

Next, the precoding is conducted. Let $\mathbf{F}_{i,SVDandGMD}$ denote the precoding matrix that based on SVD and GMD corresponding to user i proposed in this paper, more details about the $\mathbf{F}_{i,SVDandGMD}$ are presented in the Section II-B. The precoding procedure is given as follows:

$$\widetilde{\mathbf{x}}_i = \mathbf{F}_{i,SVDandGMD}\mathbf{x}_i, \tag{1}$$

where $\widetilde{\mathbf{x}}_i$ is the symbol that has been precoded.

After adding the Direct Current (DC) bias, we can obtain signal vector $\mathbf{t}$ that need to be transmitted:

$$\mathbf{t} = \sum_{i=1}^{m}(\mathbf{F}_{i,SVDandGMD}\mathbf{x}_i) + \mathbf{d}, \tag{2}$$

where m is the total number of users, $\mathbf{d}$ is the DC bias [19], and $\mathbf{t} = [\mathbf{t}_1, \ldots, \mathbf{t}_{N_t}]^T$ is the signal vector sent to each LED transmission aperture, N_t is the total number of LED transmission apertures.

B. PRECODING

As mentioned above, SVD [19] and GMD [21] can be used for precoding. For the SVD, the decomposition procedure is presented as follows:

$$\mathbf{H} = \mathbf{U}\mathbf{\Lambda}\mathbf{V}^*, \tag{3}$$

where $(\cdot)^*$ represents the conjugate transpose operation, the unitary matrix $\mathbf{U}_{N_r\times N_r}$ and the unitary matrix $\mathbf{V}_{N_t\times N_t}$ meet $\mathbf{U}^*\mathbf{U} = \mathbf{E}_{N_r\times N_r}$, $\mathbf{V}^*\mathbf{V} = \mathbf{E}_{N_t\times N_t}$, N_r is the sum of the number of LED receiving apertures $N_{r,i}$ for each user, $\mathbf{E}$ is the identity matrix, $\mathbf{\Lambda}$ is a diagonal matrix, and the elements on the diagonal are the singular values of the channel matrix $\mathbf{H}$.

In the double SVD precoding processes used in the past [19], [22], the first SVD is to decompose the complementary channel matrix $\widetilde{\mathbf{H}}_i$ of user i, and the process is as follows:

$$\widetilde{\mathbf{H}}_i = \widetilde{\mathbf{U}}_i\widetilde{\mathbf{\Lambda}}_i\left[\widetilde{\mathbf{V}}_i^{(1)} \mid \widetilde{\mathbf{V}}_i^{(0)}\right]^*. \tag{4}$$

The quasi-unitary matrix $\widetilde{\mathbf{V}}_i^{(0)}$ obtained after decomposition is used to generate the equivalent channel matrix $\overline{\mathbf{H}}_i$ of user i, the process is as follows:

$$\overline{\mathbf{H}}_{i,SVD} = \mathbf{H}_i\widetilde{\mathbf{V}}_i^{(0)} = \mathbf{U}_i\mathbf{\Lambda}\mathbf{V}_i^*, \tag{5}$$

where $\overline{\mathbf{H}}_{i,SVD}$ represents the equivalent channel matrix of user i that is decomposed by SVD, $\mathbf{H}_i$ represents the channel matrix of the user i. After generating the equivalent channel matrix, and performing the second SVD on the equivalent channel matrix, such as the (5). Then multiply the unitary matrix $\mathbf{V}_i$ decomposed by the second SVD and the quasi-unitary matrix $\widetilde{\mathbf{V}}_i^{(0)}$ decomposed by the first SVD to obtain the precoding matrix $\mathbf{F}_{i,SVD}$ of double SVD scheme, its expression is as follows:

$$\mathbf{F}_{i,SVD} = \widetilde{\mathbf{V}}_i^{(0)}\mathbf{V}_i. \tag{6}$$

On the other hand, the GMD is an extension of orthogonal triangular (QR) decomposition given as follows:

$$\mathbf{H} = \mathbf{GRQ}^*, \tag{7}$$

where the unitary matrix $\mathbf{G}_{N_r\times N_r}$ and the unitary matrix $\mathbf{Q}_{N_t\times N_t}$ also satisfy $\mathbf{G}^*\mathbf{G} = \mathbf{E}_{N_r\times N_r}$, $\mathbf{Q}^*\mathbf{Q} = \mathbf{E}_{N_t\times N_t}$. $\mathbf{R}$ is an upper triangular matrix.

In the proposed precoding scheme based on SVD and GMD in this paper, the complementary channel matrix $\widetilde{\mathbf{H}}_i$ from the transmitter of the user i is also used to first perform the SVD operation, and then uses the obtained quasi-unitary matrix $\widetilde{\mathbf{V}}_i^{(0)}$ multiplied by the user's channel matrix $\mathbf{H}_i$ to get the user's equivalent channel matrix $\overline{\mathbf{H}}_i$. However, the difference between the proposed scheme and the double SVD scheme is that GMD is used instead of SVD to decompose the user's equivalent channel matrix. This scheme has the following advantages: 1) inheriting the anti-interference performance for different users in the double SVD scheme; 2) decomposing the channel into sub-channels with the same SNR by GMD; 3) removing the complex bit allocation; so as to achieve the purpose of improving the reliability of the MU-MIMO-VLC system in this paper. Thus the process of generating the precoding matrix of the proposed scheme can be presented as follows:

$$\widetilde{\mathbf{H}}_i = \widetilde{\mathbf{U}}_i\widetilde{\mathbf{\Lambda}}_i\left[\widetilde{\mathbf{V}}_i^{(1)} \mid \widetilde{\mathbf{V}}_i^{(0)}\right]^*, \tag{8}$$

$$\overline{\mathbf{H}}_{i,GMD} = \mathbf{H}_i\widetilde{\mathbf{V}}_i^{(0)} = \mathbf{G}_i\mathbf{R}_i\mathbf{Q}_i^*, \tag{9}$$

$$\mathbf{F}_{i,SVDandGMD} = \widetilde{\mathbf{V}}_i^{(0)}\mathbf{Q}_i, \tag{10}$$

where $\overline{\mathbf{H}}_{i,GMD}$ represents the equivalent channel matrix of user i decomposed by GMD, $\mathbf{Q}_i$ is the unitary matrix component generated when the equivalent channel matrix is decomposed by GMD.

C. CHANNEL MODELS

In this subsection, we introduce the channel models [23], [24] applied in this paper. In OWC, the main factors affecting the channel response of the underwater and the atmosphere are path fading and turbulent fading, the relationship between the channel coefficient h and the two influencing factors can be expressed as follows [22]:

$$h = h_p \cdot h_t, \tag{11}$$

where h_p is path fading, h_t is turbulent fading.

The turbulence intensity is determined by the logarithmic irradiation variance σ_{It}^2. When the value is less than 1, the turbulence intensity is weak. The expression is given as follows [22]:

$$\sigma_{It}^2 = 1.23C_n^2k^{7/6}L_{au}^{11/6}, \tag{12}$$

where C_n^2 is a parameter used to describe the turbulence intensity, whose value is between 10^{-17} and 10^{-12}. k represents the phase constant, and L_{au} represents the distance of the propagation link.

In atmosphere, path loss can be divided into geometric loss and the effect of the medium on the light in the link, which can be expressed as follows [25]:

$$h_p = \frac{A}{\pi(\Theta L_{au}/2)^2}\exp(-\beta_v L_{au}), \tag{13}$$

where A is the LED receiving aperture area, Θ is the scattering angle, and β_v is the atmospheric extinction coefficient. We use Monte Carlo method (MC) [26] to model path loss in the underwater channel.

Turbulence can be divided into strong turbulence and weak turbulence. As to the turbulence loss, the log-normal distribution can be used for the weak turbulence, and the double-gamma distribution is used for modeling the strong turbulence [25]. Then the mathematical expression can be presented as [27]:

$$f(h_{t,w}) = \frac{1}{\sqrt{2\pi}\sigma_{It}h_{t,w}}\exp(-\frac{(\ln(h_{t,w}) + \sigma_{It}^2/2)^2}{2\sigma_{It}^2}), \tag{14}$$

$$f(h_{t,s}) = \frac{2(\xi\gamma)^{(\xi+\gamma)/2}}{\Gamma(\xi)\Gamma(\gamma)}h_{t,s}^{(\xi+\gamma)/2-1}B_{\xi-\gamma}(2\sqrt{\xi\gamma h_{t,s}}), \tag{15}$$

where $f(h_{t,w})$ refers to the distribution of the channel coefficient of weak turbulence $h_{t,w}$, while the $f(h_{t,s})$ means the distribution of the channel coefficient of strong turbulence $h_{t,s}$. $\Gamma(\cdot)$ is the gamma function, where $\Gamma(x) = \int_0^\infty u^{x-1}\exp^{-u}du$ [28]. The ξ, γ are the parameters describing the turbulence experienced by waves. $B_{\xi-\gamma}(\cdot)$ is the second kind of modified Bessel function [19], which order is $\xi-\gamma$, the calculation formula [28] is as follows:

$$\begin{aligned} B_{\xi-\gamma}(2\sqrt{\xi\gamma h_{t,s}}) = {} & \exp^{-(2\sqrt{\xi\gamma h_{t,s}})} \\ & \cdot(\sum_{q_1=0}^{\infty}\sum_{q_2=0}^{q_1} I(\xi-\gamma, q_1, q_2) \\ & \cdot(2\sqrt{\xi\gamma h_{t,s}})^{q_2-(2\sqrt{\xi\gamma h_{t,s}})}), \end{aligned} \tag{16}$$

$$\begin{aligned} I(\xi-\gamma, q_1, q_2) = {} & \frac{(-1)^{q_2}\sqrt{\pi}\Gamma(2(\xi-\gamma))}{2^{\xi-\gamma-q_2}\Gamma(\frac{1}{2}-(\xi-\gamma))} \\ & \times\frac{\Gamma(\frac{1}{2}+q_1-(\xi-\gamma))Z(q_1,q_2)}{\Gamma(\frac{1}{2}+q_1+(\xi-\gamma))q_1!}, \end{aligned} \tag{17}$$

$$Z(q_1, q_2) = \binom{q_1-1}{q_2-1}\frac{q_1!}{q_2!}, \tag{18}$$

where $(\cdot)!$ represents the factorial operation, $I(\cdot,\cdot,\cdot)$ is coefficients of $B_{\xi-\gamma}(\cdot)$ and involve the Lah numbers $Z(\cdot,\cdot)$ [28],

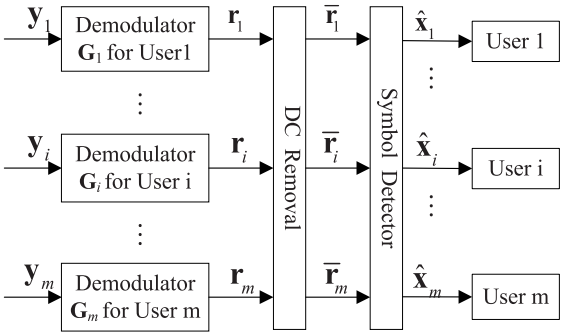

FIGURE 2. Receiver structure.

q_1, q_2 are the index of the sum in formula (16), $Z(0,0) = 1$; $Z(q_1, 0) = 0$ and $Z(q_1, 1) = q_1!$.

The expressions for ξ, γ are as follows [19]:

$$\xi = \{\exp[\frac{0.49\sigma_{It}^2}{(1+1.11\sigma_{It}^{12/5})^{7/6}}] - 1\}^{-1}, \tag{19}$$

$$\gamma = \{\exp[\frac{0.51\sigma_{It}^2}{(1+1.69\sigma_{It}^{12/5})^{5/6}}] - 1\}^{-1}. \tag{20}$$

For the air-water interface, it is well known that when light reaches an air-water interface, the refraction and reflection will occur. The wind affects the point of incidence on the plane, so the angle of refraction and the angle of incidence also change, resulting in a change in refraction. The distribution formula of polar angle [19] is as follows:

$$f(\theta_p) = \frac{2}{\sigma^2}\exp(\frac{-tan^2\theta_p}{\sigma^2})tan\theta_p sec^2\theta_p, \tag{21}$$

where θ_p is the polar angle, $\sigma^2 = 0.003 + 0.00512V$ is the mean square slope of the sea surface, and V is the wind speed. The wind speed will affect the value of σ^2, and then affect the size of the influencing pole angle, thus changing the size of the incident angle, which will cause the optical signal to be affected by temporal dispersion during transmission. According to the research data in [19] and [26], under the influence of different wind speeds, if the transmission rate of the optical signal is lower than Gbps, the influence of the time dispersion caused by the wind can be ignored in this paper.

D. RECEIVER

The structure of the receiver is shown in Fig. 2. For the MU-MIMO-VLC system, the total number of LED receiving apertures N_r is the sum of the number of LED receiving apertures $N_{r,i}$ for each user.

Similarly, for the user i, the received signal can be expressed as follows:

$$\mathbf{y}_i = \mathbf{H}_i\mathbf{t} + \mathbf{n}_i, \tag{22}$$

where $\mathbf{y}_i$ is the received signal of user i, $\mathbf{n}_i$ represents the additive noise in the channel, $\mathbf{H}_i$ is the channel matrix corresponding to user i, from Section II-B we know the channel matrix can be decomposed into three parts.

Next, applying the quasi-orthogonality of the unitary matrix to decode $\mathbf{y}_i$ that is $\mathbf{r}_i = \mathbf{G}_i^*\mathbf{y}_i$, after removing the DC bias, the expression can be expressed as follows:

$$\bar{\mathbf{r}}_i = \mathbf{R}_i\mathbf{x}_i + \mathbf{G}_i^*\mathbf{n}_i, \tag{23}$$

where $\bar{\mathbf{r}}_i$ is the symbol used by user i for Maximum Likelihood (ML) detection [10] after decoding.

Then we use the ML detection method to restore the original signal:

$$\begin{aligned}\widehat{\mathbf{x}}_i &= arg\max_{\mathbf{x}_i} p(\bar{\mathbf{r}}_i|\mathbf{x}_i, \mathbf{R}_i) \\ &= arg\min_{\mathbf{x}_i} \|\bar{\mathbf{r}}_i - \mathbf{R}_i\mathbf{x}_i\|_F^2,\end{aligned} \tag{24}$$

where $\widehat{\mathbf{x}}_i$ is the estimated symbol, $\|\cdot\|_F$ represents the norm operation.

III. PERFORMANCE ANALYSIS

In this part, we use the numerical analysis methods in [1] to derive the theoretical SER expression of the proposed scheme.

The ML detection method is used to recover the symbols, on the premise of estimating the channel matrix $\mathbf{H}$, the probability that the transmitted signal $\mathbf{x}_i$ decoded into an error code $\mathbf{x}_j$ is named as the conditional Pairwise Error Probability (PEP). The $\mathbf{x}_i - \mathbf{x}_j$ ($\mathbf{x}_i \neq \mathbf{x}_j$) means an error vector. The conditional pairwise error probability formula [1] is expressed as follows:

$$PEP = Q(\sqrt{\frac{c^2E_s}{4N_0}\|\mathbf{H}(\mathbf{x}_i - \mathbf{x}_j)\|_F^2}), \tag{25}$$

where c is the photoelectric conversion coefficient and in this paper is 1, E_s means the signal energy, while the N_0 is the noise power, and $Q(\cdot)$ is the error complementary function.

Next we derive the conditional pairwise error probability of the scheme as below:

$$PEP(\mathbf{x}_i \longrightarrow \mathbf{x}_j|\mathbf{R}) = Q(\sqrt{\frac{\eta\|\mathbf{R}(\mathbf{x}_i - \mathbf{x}_j)\|_F^2}{4}}), \tag{26}$$

where $\eta = \frac{E_s}{N_0}$ represents the SNR.

Then we use the traversal method to obtain the minimum Euclidean distance and substitute it into the above formula, and average the conditional pairwise error probability of all transmission signals, the lower bound of the conditional pairwise error probability can be obtained as [22]:

$$PEP(e|\mathbf{R}, \mathbf{x}_i) = \frac{1}{S}\sum_{i=1}^{S} Q(\sqrt{\frac{\eta \cdot \min\limits_{i\neq j}\|\mathbf{R}(\mathbf{x}_i - \mathbf{x}_j)\|_F^2}{4}}), \tag{27}$$

where S indicates that the symbols that the receiver can receive by the traversal method.

We use the method of the numerical analysis to approximate the integral summation of the (27) to obtain the lower bound of the theoretical SER of the proposed scheme [19]:

$$P_{e,l} \approx \frac{1}{W}\sum_{w=1}^{W} PEP(e|\mathbf{R}_w, \mathbf{x}_i), \tag{28}$$

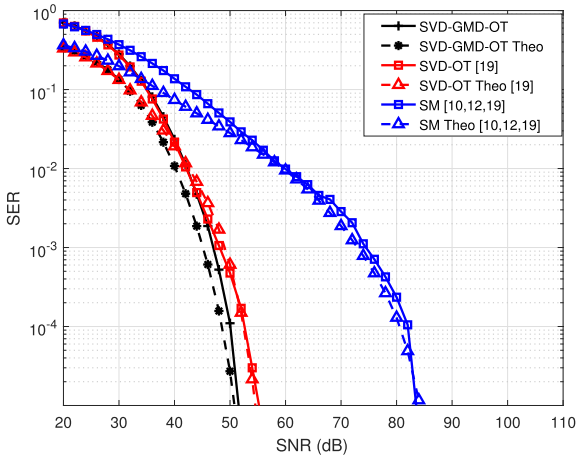

FIGURE 3. Theoretical and simulation comparisons in the atmosphere, $\sigma_{It}^2 = 0.2614$.

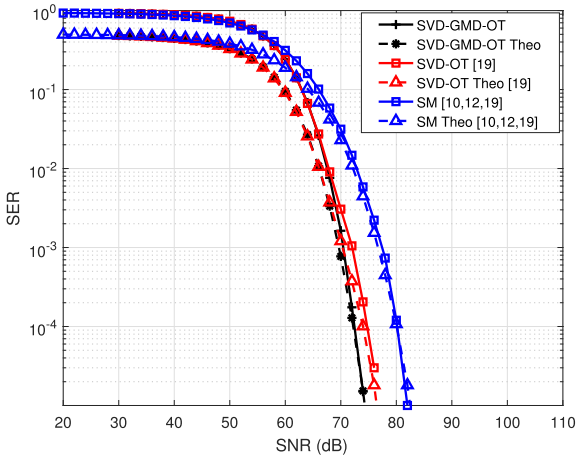

FIGURE 4. Theoretical and simulation results in the underwater, $\sigma_{It}^2 = 0.0734$.

where W indicates that W samples are used in the approximation using the numerical analysis, w is index number.

IV. SIMULATION

In this section, we first compare the simulation SER and theoretical SER of the SVD-GMD-OT scheme in this paper to verify the effectiveness of the proposed scheme. Then we compare the SER of the SVD-GMD-OT scheme in this paper with two benchmark schemes that are SM [10], [12], [19] scheme and Double SVD assisted OT (SVD-OT) [19] scheme in atmosphere, underwater and air-water interface channels to verify that the proposed scheme in this paper can effectively improve the reliability of the MU-MIMO-VLC system. In addition, SER of air-water interface, underwater channel and atmospheric channel under different wind speed, water quality and propagation distance were simulated to demonstrate the influence of the three factors on the reliability of the scheme proposed in this paper.

In the simulation, we assume that relatively perfect channel state information can be obtained. There are two users, each user has two LED transmission apertures and two LED receiving apertures, and other fixed simulation environments are as follows.

In our simulation, we assume that the light source is a laser with a beam width of 3mm and a beam wavelength of 550nm. We set the photoelectric conversion efficiency c as 1 and the field of view (FOV) semi-angle of receiver as $\Psi_{1/2} = 45°$. Also we set the LED receiving aperture diameter as $D = 0.05$m and the divergence semi-angle of transmitters as $\Phi_{1/2} = 0.5°$. Then the separation distance between receivers is set as $s_r = 0.25$m, and the separation distance between transmitters is set as $s_t = 0.25$m.

Fig. 3 and Fig. 4 show the theoretical and simulation SER respectively in atmospheric and underwater scenarios. We assume that $\sigma_{It}^2 = 0.2614$ in the atmosphere and $\sigma_{It}^2 = 0.0734$ in the underwater, wherein the atmospheric propagation link is 600m, and the underwater propagation link is 300m. From the comparison results, we can see that with the increase of the SNR, the simulation and theoretical SER curves are basically consistent. Moreover, it can be found that the SER performance of the scheme proposed in this paper is superior to SER performance of SVD-OT scheme and SM scheme, indicating that the reliability of the scheme proposed in this paper is superior to the reliability of SVD-OT scheme and SM scheme.

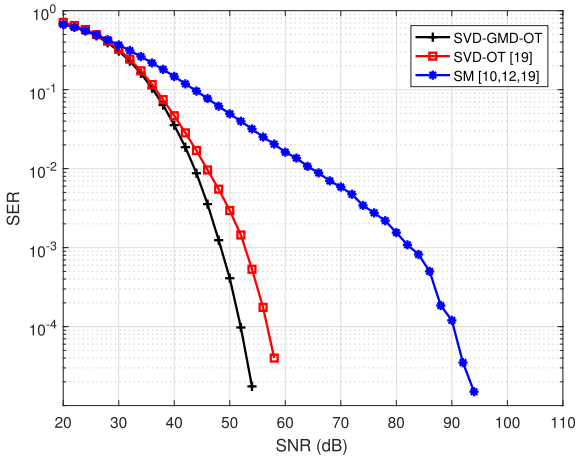

FIGURE 5. Comparison of three schemes in the case of strong turbulence in the atmosphere, $\sigma_{It}^2 = 1.4024$.

TABLE 1. The percentage SER of three schemes in the atmosphere.

	SER		
SNR(dB)	SVD-GMD-OT	SVD-OT	SM
46	0.355%	0.962%	7.721%
48	0.124%	0.550%	6.171%
50	0.041%	0.295%	4.941%
52	0.010%	0.145%	3.982%
54	0.002%	0.053%	3.184%
56	0.000%	0.018%	2.513%

Fig. 5 shows the comparison of the three schemes including the scheme proposed in this paper, SVD-OT and SM in the

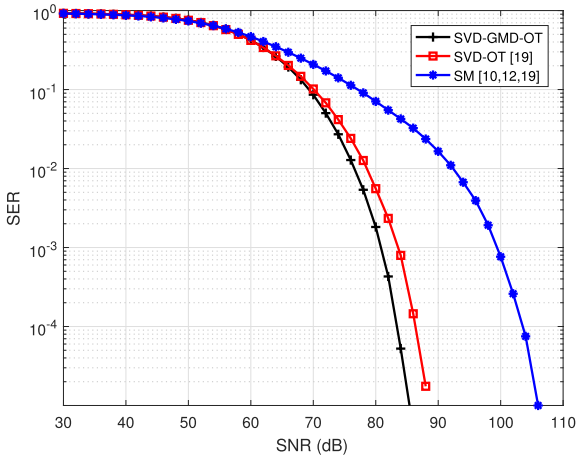

FIGURE 6. Comparison of three schemes in the case of strong turbulence in the underwater, $\sigma_{It}^2 = 1.1401$.

atmospheric channel, wherein the turbulence is strong with $\sigma_{It}^2 = 1.4024$, and the propagation link is 1500m. As can be seen from the figure, with the increase of the SNR, the scheme proposed in this paper has improved the SER performance, while the SER performance of the proposed scheme in this paper is superior to the SER performance of the SVD-OT scheme and the SM scheme.

From Table 1 obtained in Fig. 5, it can be seen that the percentage SER of the proposed scheme in this paper is much smaller than the percentage SER of the SVD-OT scheme and SM scheme, which proves that the SER performance of the proposed scheme in this paper is better than that of the SVD-OT scheme and SM scheme, so the proposed scheme in this paper can effectively improve the reliability of the MU-MIMO-VLC system. In the same case, Fig. 3 compares the reliability when the turbulence is weak with $\sigma_{It}^2 = 0.2614$. Through SER comparison, it can be seen that the reliability of the proposed scheme in this paper is better than the reliability of SVD-OT scheme and SM scheme.

Then we compare the SER performance of the three schemes over the underwater channel when the strong turbulence satisfies $\sigma_{It}^2 = 1.1401$, and the propagation link is 1340m. As shown in Fig. 6, the composition of substances in water is related to the type of water, such as clear water, coastal water and harbor water. Compared with atmosphere, because the stones, sand and other aerosol substances contained in clear water or coastal water or harbor water will have a great impact on the absorption and scattering of light. So light transmission is more affected underwater than in the atmosphere. So the SER performance of each scheme is worse than those in the atmosphere. However, it can also be seen that under strong turbulence, the SER performance of the proposed scheme in this paper is better than that of SVD-OT scheme and SM scheme.

It can also be seen from Table 2 obtained in the Fig. 6 that with the increase of SNR, the percentage SER of the proposed scheme in this paper is much smaller than that of the SVD-OT scheme and the SM scheme. So the SER performance of

TABLE 2. The percentage SER of three schemes in the underwater.

	SER		
SNR(dB)	SVD-GMD-OT	SVD-OT	SM
74	2.715%	4.163%	14.063%
76	1.281%	2.408%	11.322%
78	0.538%	1.264%	9.072%
80	0.182%	0.556%	7.077%
82	0.043%	0.234%	5.485%
84	0.005%	0.08%	4.251%

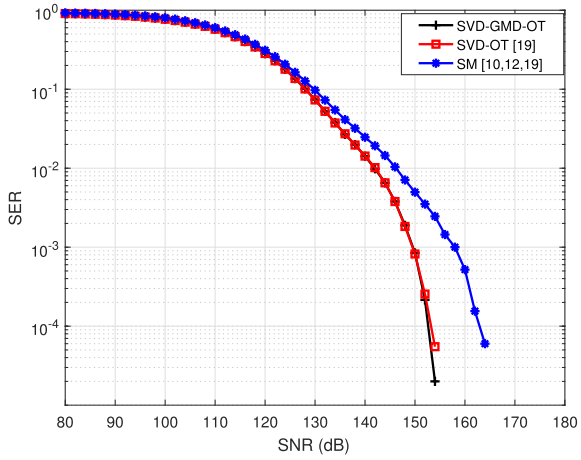

FIGURE 7. Comparison of three schemes in the air-water interface, $C_n^2 = 10^{-14}$.

TABLE 3. The percentage SER of three schemes in the air-water interface.

	SER		
SNR(dB)	SVD-GMD-OT	SVD-OT	SM
144	0.652%	0.653%	1.448%
146	0.379%	0.379%	1.04%
148	0.189%	0.183%	0.71%
150	0.085%	0.082%	0.498%
152	0.022%	0.026%	0.351%
154	0.002%	0.006%	0.246%

the proposed scheme in this paper is always better than that of the SVD-OT scheme and the SM scheme. Thus proving that the scheme proposed in this paper can still improve the reliability of the MU-MIMO-VLC system under water, and its reliability is better than the other two benchmark schemes. In the same case, for underwater where the turbulence intensity satisfies $\sigma_{It}^2 = 0.0734$ and the propagation link is 300m in Fig. 4, the reliability of the scheme proposed in this paper is still superior to the reliability of the SVD-OT scheme and SM scheme.

Moreover, we compared the SER performance of three schemes, when the wind speed is 1m/s, the atmospheric propagation link is 1500m, the underwater propagation link is 1340m, and $C_n^2 = 10^{-14}$ in the air-water interface environment, such as Fig. 7 and Table 3.

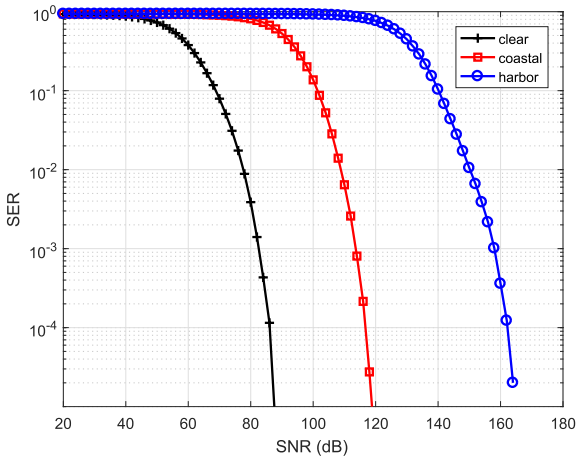

FIGURE 8. SER performance of the proposed system in the underwater with different water quality.

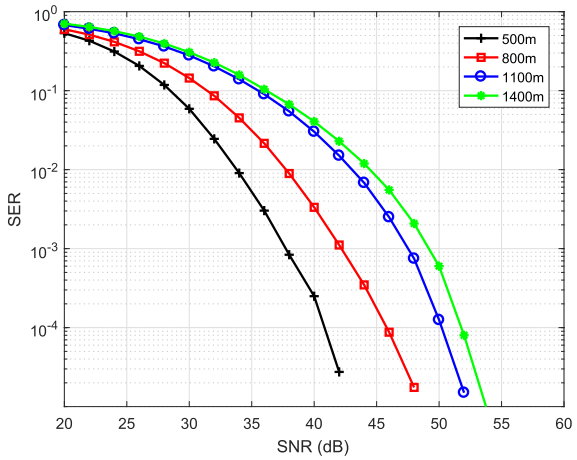

FIGURE 9. SER performance of the proposed system in the atmosphere with different link distances.

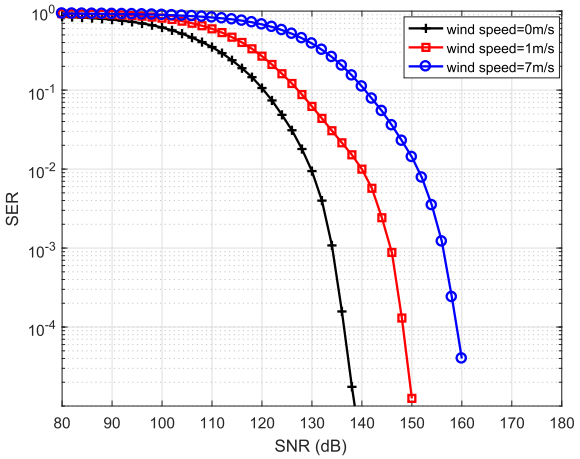

FIGURE 10. SER performance of the proposed system in the air-water interface with different wind speeds.

In the case of small SNR, the SER performance of the proposed scheme in this paper is almost the same as the SER performance of the SVD-OT scheme, such as Fig. 7. This is because the underwater propagation environment is worse than that in the atmosphere, the light that travels underwater is just refracted light and the SNR is small. Even though GMD can decompose the channel into sub-channels with the same SNR, the performance improvement of the proposed scheme in this paper is not obvious due to excessive noise.

However, after SNR greater than 150dB, with the increase of SNR, because GMD divides the channel into sub-channels with the same SNR, the channel propagation condition is better than that of double SVD scheme, the SER performance of the proposed scheme in this paper is better than that of the SVD-OT scheme, for example, when SNR is greater than 150dB in Table 3.

Moreover, in Fig. 7 and Table 3, the SER performance of the proposed scheme in this paper is far superior to the SER performance of the SM scheme. This is because the proposed scheme in this paper inherits the advantage of the double SVD scheme to resist interference between different users and inherits the advantage which brought by GMD that decomposing the channel into subchannels with the same SNR.

It can be seen from the simulation results in Fig. 3 to Fig. 7 and Table 1 to Table 3 that the precoding scheme proposed in this paper can effectively improve the reliability of the system.

Fig. 8 shows the SER performance of the proposed scheme in this paper under the conditions of different water quality. It can be seen from the figure that the propagation in clear water requires a lower SNR. From the SER conditions of different water quality, we can conclude that the more underwater influencing factors, the reliability of the system will decrease.

Fig. 9 shows the SER performance of the proposed scheme in this paper in the atmosphere with the different link distances: 500m, 800m, 1100m and 1400m. As can be seen from the figure, as the link distance increases, the SNR required for propagation is also higher. The simulation results also prove that the link distance is larger, the reliability of the system will decrease.

Fig. 10 shows the SER performance of the proposed scheme in this paper in the air-water interface environment with different wind speed: 0m/s, 1m/s and 7m/s. As can be seen from the figure, as the wind speed increases, the SNR required for propagation becomes higher, the system reliability decreases.

V. CONCLUSION

In this paper, we propose a precoding scheme based on SVD and GMD to improve the reliability of MU-MIMO-VLC system. In this design, the user data are first modulated and encoded by PAM and OT. Then SVD and GMD are conducted to generate the precoding matrix. The precoded symbols are delivered via multiple LED apertures. At the receiver, perform the corresponding demodulation operation. After that, the theoretical SER is derived. The scheme proposed in this paper has the following advantages: 1) inheriting the

anti-interference performance for different users in the double SVD scheme; 2) decomposing the channel into sub-channels with the same SNR by GMD; 3) removing the complex bit allocation; thereby improving the reliability of the MU-MIMO-VLC system. Moreover, the simulation results verify the effectiveness of the SVD-GMD-OT scheme and show that the SER performance of the SVD-GMD-OT scheme is better than the SER performance of the benchmark schemes, thus proving that the proposed scheme can effectively improve the reliability of MU-MIMO-VLC system. Therefore, the precoding scheme based on SVD and GMD proposed in this paper can be applied to the MU-MIMO-VLC system to improve the reliability of the system. However, the optical signal in the MU-MIMO-VLC system is easy to be stolen, so it is hoped that the security of its physical layer can be improved in the future.

REFERENCES

[1] T. Fath and H. Haas, "Performance comparison of MIMO techniques for optical wireless communications in indoor environments," *IEEE Trans. Commun.*, vol. 61, no. 2, pp. 733–742, Feb. 2013.

[2] S. Mumtaz, J. Rodriguez, and L. Dai, *mmWave Massive MIMO: A Paradigm for 5G*, 2016.

[3] W. Feng, Y. Wang, D. Lin, N. Ge, J. Lu, and S. Li, "When mmWave communications meet network densification: A scalable interference coordination perspective," *IEEE J. Sel. Areas Commun.*, vol. 35, no. 7, pp. 1459–1471, Jul. 2017.

[4] B. Wang, L. Dai, Z. Wang, N. Ge, and S. Zhou, "Spectrum and energy-efficient beamspace MIMO-NOMA for millimeter-wave communications using lens antenna array," *IEEE J. Sel. Areas Commun.*, vol. 35, no. 10, pp. 2370–2382, Oct. 2017.

[5] X. Li, T. Jiang, S. Cui, J. An, and Q. Zhang, "Cooperative communications based on rateless network coding in distributed MIMO systems [coordinated and distributed MIMO]," *IEEE Wireless Commun.*, vol. 17, no. 3, pp. 60–67, Jun. 2010.

[6] Z. Xiao, P. Xia, and X. G. Xia, "Enabling UAV cellular with millimeter-wave communication: Potentials and approaches," *IEEE Commun. Mag.*, vol. 54, no. 5, pp. 66–73, May 2016.

[7] J. Zhang, Y. Zhang, Y. Yu, R. Xu, Q. Zheng, and Z. Ping, "3-D MIMO: How much does it meet our expectations observed from channel measurements?" *IEEE J. Sel. Areas Commun.*, vol. 35, no. 8, pp. 1887–1903, Aug. 2017.

[8] N. Solomennikova, A. Sherstobitov, and V. Lyashev, "Frequency selective MIMO precoding in time domain," in *Proc. Int. Conf. Eng. Telecommun. (En&T)*, 2021, pp. 1–6.

[9] R. F. Siregar, N. Rajatheva, and M. Latva-Aho, "Permutation channel modulation: New index modulation mechanism for MIMO," in *Proc. IEEE 93rd Veh. Technol. Conf.*, Apr. 2021, pp. 1–6.

[10] S. B. Patel, D. V. Chauhan, and J. D. Patel, "Spatial modulation: Challenges and potential solutions," in *Proc. Int. Conf. Smart Gener. Comput., Commun. Netw. (SMART GENCON)*, Oct. 2021, pp. 1–8.

[11] Z. Li, W. Gao, M. Zhang, and J. Xiong, "Multi-task deep learning based hybrid precoding for mmWave massive MIMO system," *China Commun.*, vol. 18, no. 10, pp. 96–106, 2021.

[12] S. Naser, L. Bariah, S. Muhaidat, M. Al-Qutayri, M. Uysal, and P. C. Sofotasios, "Space-time block coded spatial modulation for indoor visible light communications," *IEEE Photon. J.*, vol. 14, no. 1, pp. 1–11, Feb. 2022.

[13] T. Komine and M. Nakagawa, "Fundamental analysis for visible-light communication system using LED lights," *IEEE Trans. Consum. Electron.*, vol. 50, no. 1, pp. 100–107, Feb. 2004.

[14] D. C. O'Brien, "Visible light communications: Challenges and possibilities," in *Proc. Photon. Conf.*, 2011.

[15] N. Huang, X. Wang, and C. Ming, "Transceiver design for MIMO VLC systems with integer-forcing receivers," *IEEE J. Sel. Areas Commun.*, vol. 36, no. 1, pp. 66–77, Jan. 2018.

[16] H. Kaushal and G. Kaddoum, "Underwater optical wireless communication," *IEEE Access*, vol. 4, pp. 1518–1547, 2016.

[17] S. Hranilovic, *Wireless Optical Communication Systems*. New York, NY, USA: Springer, 2005.

[18] L. Zeng, D. C. O'Brien, H. L. Minh, G. E. Faulkner, K. Lee, D. Jung, Y. Oh, and T. E. Won, "High data rate multiple input multiple output (MIMO) optical wireless communications using white LED lighting," *IEEE J. Sel. Areas Commun.*, vol. 27, no. 9, pp. 1654–1662, Dec. 2009.

[19] G. Huang, L. Zhang, Y. Jiang, and Z. Wu, "A general orthogonal transform aided MIMO design for reliable maritime visible light communications," *J. Lightw. Technol.*, vol. 38, no. 23, pp. 6549–6560, Dec. 1, 2020.

[20] K. Cai and M. Jiang, "SM/SPPM aided multiuser precoded visible light communication systems," *IEEE Photon. J.*, vol. 8, no. 2, pp. 1–9, Apr. 2016.

[21] T. Xie, L. Dai, X. Gao, M. Z. Shakir, and J. Li, "Geometric mean decomposition based hybrid precoding for millimeter-wave massive MIMO," *China Commun.*, vol. 15, no. 5, pp. 229–238, 2018.

[22] G. Huang and L. Zhang, "Reliable rotation transform aided MIMO scheme for underwater visible light communication," in *Proc. IEEE/CIC Int. Conf. Commun. China (ICCC)*, Aug. 2019, pp. 989–993.

[23] Y. Kaymak, R. Rojas-Cessa, J. Feng, N. Ansari, M. Zhou, and T. Zhang, "A survey on acquisition, tracking, and pointing mechanisms for mobile free-space optical communications," *IEEE Commun. Surveys Tuts.*, vol. 20, no. 2, pp. 1104–1123, 2nd Quart., 2018.

[24] S. Han, Y. Noh, R. Liang, R. Chen, Y.-J. Cheng, and M. Gerla, "Evaluation of underwater optical-acoustic hybrid network," *China Commun.*, vol. 11, no. 5, pp. 49–59, 2014.

[25] A. Mishra, P. S. Pati, and R. K. Giri, "Performance analysis of SIM based FSO using various modulation techniques with APD receiver over turbulent channel," in *Proc. Int. Conf. Wireless Commun., Signal Process. Netw. (WiSPNET)*, 2017, pp. 2730–2734.

[26] C. Gabriel, M. A. Khalighi, S. Bourennane, P. Leon, and V. Rigaud, "Channel modeling for underwater optical communication," in *Proc. IEEE Globecom Workshops*, Dec. 2011, pp. 833–837.

[27] D. A. Luong, T. C. Thang, and A. T. Pham, "Effect of avalanche photodiode and thermal noises on the performance of binary phase-shift keying-subcarrier-intensity modulation/free-space optical systems over turbulence channels," *IET Commun.*, vol. 7, no. 8, pp. 738–744, Mar. 2013.

[28] M. M. Molu, P. Xiao, M. Khalily, L. Zhang, and R. Tafazolli, "A novel equivalent definition of modified Bessel functions for performance analysis of multi-hop wireless communication systems," *IEEE Access*, vol. 5, pp. 7594–7605, 2017.

WENDUO QIU received the B.S. degree from the School of Information Science and Engineering, Henan University of Technology, Zhengzhou, China, in 2020. He is currently pursuing the master's degree with the School of Information Science and Technology, Tibet University. His main research interests include security and reliability of communication systems.

YAN FENG received the B.S. degree from Tibet University, China, in 2003 and the M.S. degree from Southwest Jiaotong University, China, in 2010. He is currently an Associate Professor with Tibet University. His research interests include signal and information processing and machine learning.

YOU ZHANG received the B.S. degree from the Huaiyin Institute of Technology, China, in 2019. She is currently pursuing the master's degree with the School of Information Science and Technology, Tibet University, China. Her research interest includes communication system reliability.